Ocular Drug Delivery Nanowafer with Enhanced Therapeutic Efficacy

Xiaoyong Yuan,[†] Daniela C. Marcano, Crystal S. Shin, Xia Hua,[†] Lucas C. Isenhart, Stephen C. Pflugfelder,[*] and Ghanashyam Acharya[*]

Ocular Surface Center, Cullen Eye Institute, Department of Ophthalmology, Baylor College of Medicine, One Baylor Plaza, Houston, Texas 77030, United States. [†]Present address: Tianjin Eye Hospital, Clinical College of Ophthalmology, Tianjin Medical University, Tianjin, China 300020.

ABSTRACT Presently, eye injuries are treated by topical eye drop therapy. Because of the ocular surface barriers, topical eye drops must be applied several times in a day, causing side effects such as glaucoma, cataract, and poor patient compliance. This article presents the development of a nanowafer drug delivery system in which the polymer and the drug work synergistically to elicit an enhanced therapeutic efficacy with negligible adverse immune responses. The nanowafer is a small transparent circular disc that contains arrays of drug-loaded nanoreservoirs. The slow drug release from the nanowafer increases the drug residence time on the ocular surface and its subsequent absorption into the surrounding ocular tissue. At the end of the stipulated period of drug release, the nanowafer will dissolve and fade away. The *in vivo* efficacy of the axitinib-loaded nanowafer was demonstrated in treating corneal neovascularization (CNV) in a murine ocular burn model. The laser scanning confocal imaging and RT-PCR study revealed that once a day administered axitinib nanowafer was therapeutically twice as effective, compared to axitinib delivered twice a day by topical eye drop therapy. The axitinib nanowafer is nontoxic and did not affect the wound healing and epithelial recovery of the ocular burn induced corneas. These results confirmed that drug release from the axitinib nanowafer is more effective in inhibiting CNV compared to the topical eye drop treatment even at a lower dosing frequency.

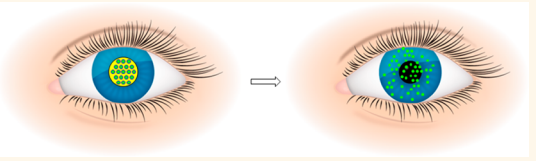

KEYWORDS: nanowafer · drug delivery · inflammation · corneal neovascularization · therapeutic efficacy

Eye injuries are one of the major causes of blindness worldwide, and in the United States alone 2.5 million eye injuries occur every year.[1] Ocular surface injuries disrupt corneal angiogenic privilege and trigger corneal neovascularization (CNV), eventually leading to loss of vision.[2] Ocular drug delivery, although it may seem to be deceptively simple, is a challenging task mainly because of the unique barriers associated with the ocular surface that impede adequate drug delivery and therapeutic efficacy.[3] Topical drug therapy with eye drop formulations is the most accessible and noninvasive. However, its potential is limited by the ocular surface protective barriers, such as reflex tearing, constant blinking, impervious nature of the ocular surface due to tight epithelial junctions, and nasolacrimal drainage that can rapidly clear the eye drops from the ocular surface in a few minutes.[4,5] In addition, drug clearance due to systemic absorption through blood capillaries in the conjunctival sac can further reduce the amount of drug available for effective ocular absorption.[6,7] These physiological barriers contribute to inadequate drug delivery and reduced bioavailability of the drug to the eye. Hence, topical eye drops must be applied several times a day, thus increasing the potential for toxic side effects such as cellular damage, inflammation of the ocular surface, and temporary blurred vision, leading to discomfort and poor patient compliance.[8,9] Topical eye drop therapies that target CNV often produce side effects such glaucoma and cataract formation.[10,11]

To improve treatment efficacy, emulsions, liposomes, micelles, and nanoparticle suspensions have been used in ocular drug delivery. However, these formulations were also rapidly cleared from the eye.[12−15] *In situ* gel-forming systems have been developed for ocular drug delivery.[16] A hydrogel-forming solution containing drug upon instillation as eye drops undergoes sol-to-gel phase transition on the eye surface. The *in situ*-formed gels are expected to hold the drug for a longer period of time, thus enhancing its bioavailability. However, these formulations are also quickly cleared

* Address correspondence to gacharya@bcm.edu, stevenp@bcm.edu.

Received for review November 19, 2014 and accepted January 13, 2015.

Published online 10.1021/nn506599f

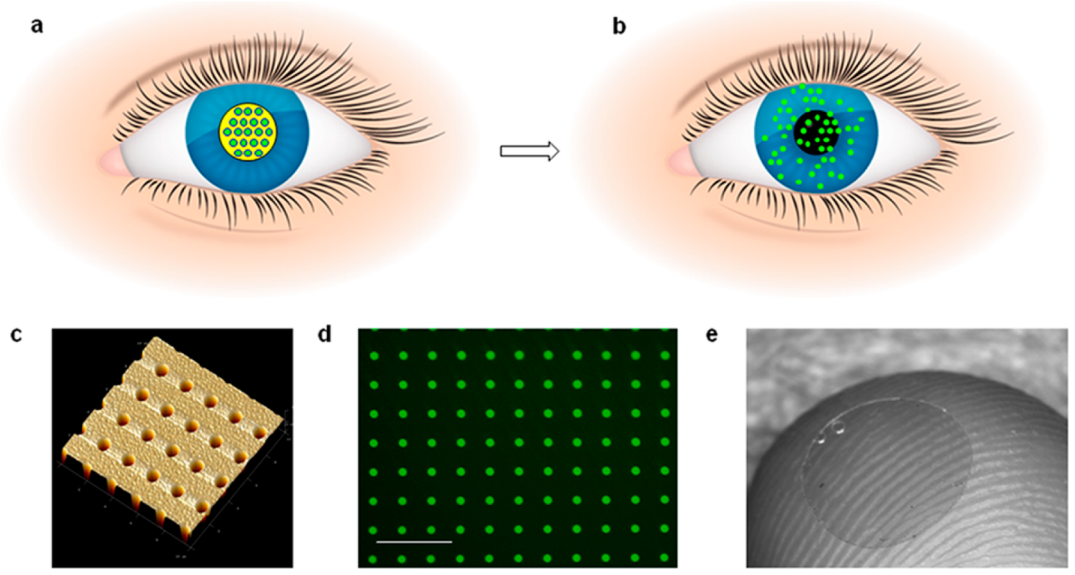

Figure 1. Ocular drug delivery nanowafer. (a) Schematic of the nanowafer instilled on the cornea. (b) Diffusion of drug molecules into the corneal tissue. (c) AFM image of a nanowafer demonstrating an array of 500 nm diameter nanoreservoirs. (d) Fluorescence micrograph of a nanowafer filled with doxycycline (scale bar 5 μm). (e) Nanowafer on a fingertip.

from the ocular surface, resulting in limited therapeutic efficacy. Drug-loaded contact lenses have been developed to improve the drug retention time in the eye.[17,18] All these systems could not release the drug for extended periods of time, leading to limited drug efficacy, thus requiring multiple administrations.

In this context, development of a novel nano drug delivery system that can surmount the ocular surface barriers and release the drug for extended periods of time, thus enhancing therapeutic efficacy and improving patient compliance, is vitally important to treat ocular injuries, infections, and inflammatory conditions and restore normal physiological functions of the eye.

RESULTS AND DISCUSSION

This article presents the development of an ocular drug delivery nanowafer, wherein the drug carrying polymer and the drug work synergistically to provide an augmented therapeutic effect compared to conventional eye drop therapy. The nanowafer is a tiny transparent circular disc that can be applied on the ocular surface with a fingertip and can withstand constant blinking without being displaced (Figure 1). It contains arrays of drug-loaded nanoreservoirs from which the drug will be released in a tightly controlled fashion for a few hours to days. The slow drug release from the nanowafer increases the drug residence time on the ocular surface and its subsequent absorption into the surrounding ocular tissue. At the end of the stipulated period of drug release, the nanowafer will dissolve and fade away. The development of an ocular drug delivery nanowafer and its enhanced *in vivo* therapeutic efficacy is herein demonstrated by treating corneal neovascularization in a murine ocular burn (OB) model.[19]

Nanowafer Fabrication. In this study, four different polymers, poly(vinyl alcohol) (PVA), polyvinylpyrrolidone (PVP), (hydroxypropyl)methyl cellulose (HPMC), and carboxymethyl cellulose (CMC), were used for nanowafer fabrication. These polymers were selected for their water solubility, biocompatibility, mucoadhesivity, transparency, and film-forming properties so as to readily adhere to a wet mucosal surface and conform to the curvature of the eye.[20] Aqueous solutions of these polymers are currently in clinical use as artificial tears, and therefore nanowafers fabricated with these polymers can function both as a drug delivery system and also as lubricant.[21,22] The nanowafers were fabricated *via* the hydrogel template strategy with a few modifications (Figure 2).[23,24] The first step involves the fabrication of arrays of wells (500 nm diameter and 500 nm depth) on a silicon wafer by e-beam lithography followed by preparation of its poly(dimethylsiloxane) (PDMS) imprint. In the second step, a polymer solution will be poured on the PDMS template followed by baking. The polymer wafer containing 500 nm diameter wells was peeled off and placed on the flat surface to expose the wells. The wells in the polymer wafer were filled with a solution of drug/polymer mixture. In this study, blank nanowafers (without the drug) of PVA, PVP, HPMC, and CMC and PVA nanowafers loaded with sunitinib, sorafenib, axitinib, and doxycycline were fabricated.

Immunostimulatory Properties of Nanowafers. The inflammatory response to injury is important to recovery, but if dysregulated can enhance tissue damage, stimulate angiogenesis, disrupt healing, and cause corneal opacity.[25,26] Since the cornea is optically clear and avascular, its neovascularization and opacification result in eventual loss of vision. The biopolymers

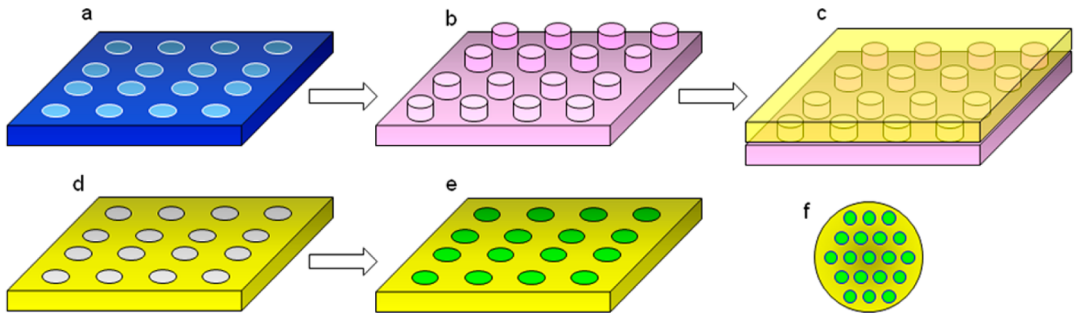

Figure 2. Schematic of nanowafer fabrication. (a) Silicon wafer master template having 500 nm wells fabricated by e-beam lithography. (b) PDMS imprint containing vertical posts. (c) Fabrication of a PVA template. (d) PVA template. (e) PVA template filled with drug. (f) Drug-filled nanowafer.

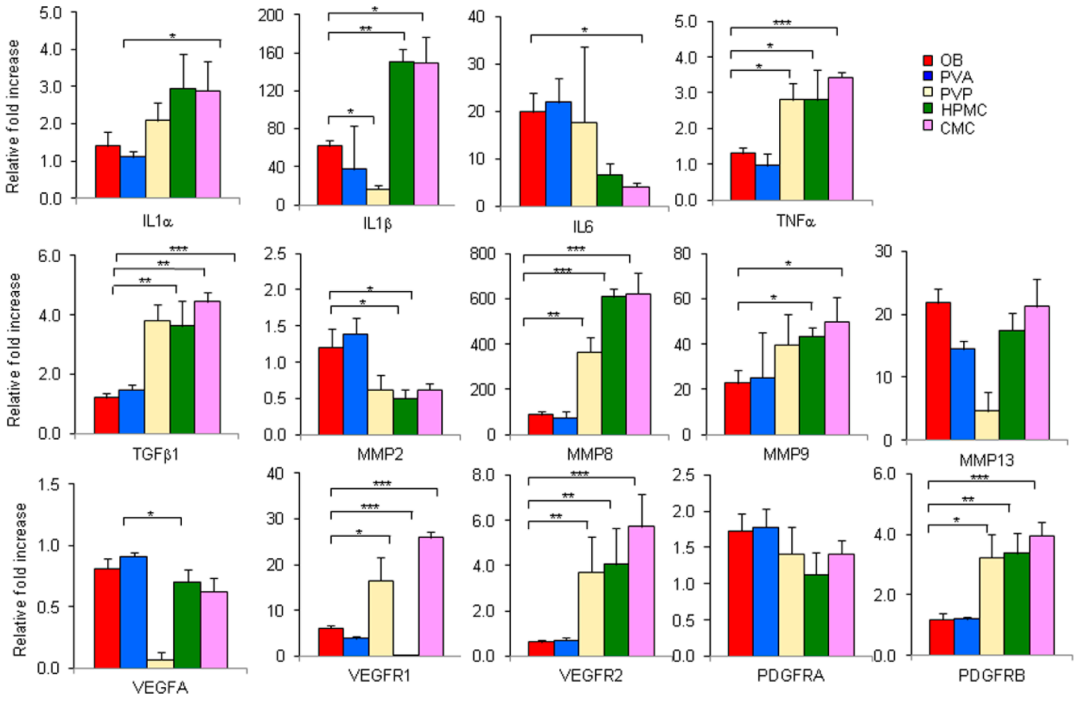

Figure 3. Poly(vinyl alcohol) nanowafer is nonimmunogenic. RT-PCR analysis confirming that PVA nanowafers do not induce upregulation of proinflammatory and proangiogenic factors. $n = 3$ (5 animals per group), $^{*}P < 0.05$, $^{**}P < 0.01$, $^{***}P < 0.001$). All error bars represent standard deviation from the mean.

used in the nanowafer fabrication is crucial, as they can be immunostimulatory, *i.e.*, can induce inflammation and exacerbate the condition, leading to delayed wound healing and incomplete recovery.[27−29] Choosing the right biopolymer that is nonstimulatory to the cornea's immunological and inflammatory responses and that improves the tolerability, stability, and therapeutic effect of the drug with minimal side effects is vital for the success of the ocular drug delivery nanowafer.

As a first step, a quantitative analysis of the ability of the polymers to elicit proinflammatory and proangiogenic responses in an OB mouse model was developed. The polymer nanowafers (tiny circular discs of 2 mm diameter and 100 μm thickness) were instilled on the corneas of OB-induced mice, daily for 5 days. At the end of the treatment period, the corneas were collected and processed for evaluating proinflammatory and proangiogenic genes by reverse transcription polymerase chain reaction (RT-PCR) analysis.

During the wound-healing process, the expression levels of several proinflammatory interleukins, IL-1α, IL-1β, and IL-6, tumor necrosis factor TNF-α, and proangiogenic matrix metalloproteinases MMP-2, MMP-8, MMP-9, and MMP-13, and transforming growth factor TGF-β1 will be upregulated.[30−33] Quantification of the expression levels of these factors gives insights into the effect of polymer materials on inflammation and angiogenesis. In this study, proinflammatory and proangiogenic attributes of PVA, PVP, HPMC, and CMC nanowafers were evaluated in the corneas after injury by RT-PCR analysis (Figure 3). The PVA nanowafers were nonstimulatory, and the expression levels of proinflammatory factors were almost equal to the OB control group, while the PVP, HPMC, and CMC nanowafers significantly upregulated the expression of

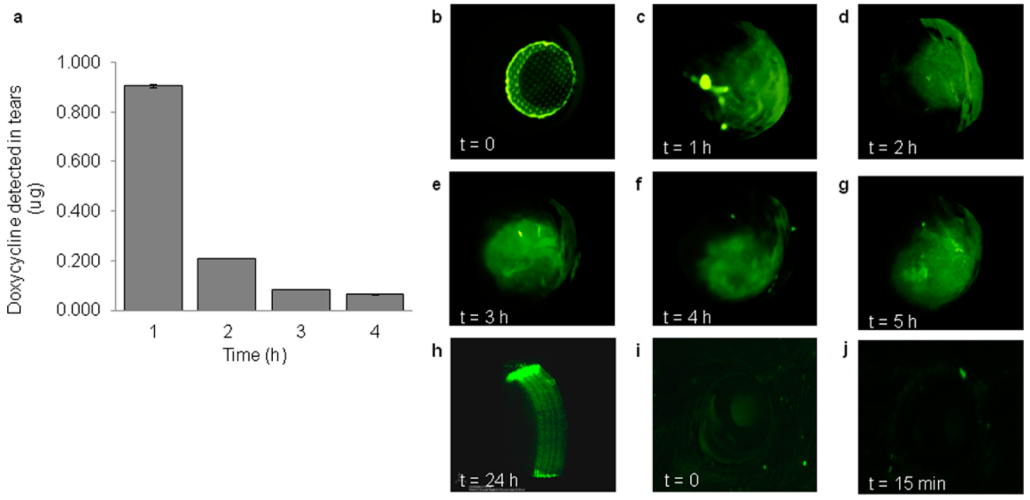

Figure 4. Nanowafer drug delivery enhances drug molecular transport into the cornea. (a) *In vivo* drug release from a doxycycline nanowafer placed on the cornea and measurement of the drug concentration in tears. (b–g) Fluorescence stereomicroscopic images of mouse cornea at regular time intervals demonstrating the doxycycline release from the nanowafer into the cornea. (h) Intravital confocal fluorescence image of the mouse eye showing the presence of doxycycline at 24 h. (i and j) Rapid clearance of doxycycline eye drops in 15 min in mice.

one or more inflammatory cytokines (IL-1α, IL-1β, and TNF-α) compared to the OB control group. The PVP, HPMC, and CMC nanowafers stimulated the expression levels of MMP-8, MMP-9, and TGF-β1, while the PVA nanowafers were nonstimulatory, and the expression levels of these factors were very close to the OB control group.

The polymer nanowafers were further investigated for their effect on the expression levels of proangiogenic vascular endothelial growth factor A (VEGF-A), tyrosine kinase receptors VEGF-R1 and VEGF-R2, and platelet-derived growth factor receptors (PDGFR-A and PDGFR-B). The PVA nanowafer has a nonstimulatory effect on the expression levels of these factors, and they remain very close to the OB control group. However, all other polymer nanowafers have upregulated VEGF-R1, VEGF-R2, and PDGFR-B expression levels. Taken together, these results indicate that PVA nanowafers are well tolerated by the ocular surface and do not stimulate the expression of proinflammatory and proangiogenic factors. To take advantage of these attributes, PVA was chosen for the fabrication of nanowafers. Furthermore, these results also indicate that the PVA nanowafers are well suited for the delivery of antiangiogenic small molecular tyrosine kinase receptor inhibitor (TKI) drugs to treat CNV.

Nanowafer Enhances Drug Diffusion into the Cornea. To demonstrate the ability of the nanowafers to release the drug for an extended period of time, PVA nanowafers loaded with doxycycline were fabricated. Doxycycline (antibiotic drug) was chosen for this study because of its green fluorescence, which allowed us to monitor the precorneal drug residence time and its subsequent diffusion into the cornea by real-time fluorescence imaging.[34] To monitor the drug concentration on the ocular surface as a measure of drug release from the nanowafer, tear samples were collected hourly for 5 h, and the doxycycline content was analyzed by HPLC.[35] After placement of a doxycycline nanowafer on the cornea, the drug concentration in the tears slowly decreased with time, and after 4 h, no detectable doxycycline concentration was present (Figure 4a). To monitor the drug diffusion into the mouse cornea after the instillation of a doxycycline nanowafer, it was subjected to fluorescence imaging at hourly intervals under general anesthesia. The corneas were green fluorescent even after 5 h when viewed under a stereomicroscope with 488 nm illumination, indicating the presence of drug in the cornea (Figure 4b–g). The corneas exhibited a strong green fluorescence even after 24 h, when subjected to intravital laser scanning confocal imaging, indicating the presence of doxycycline in the corneal tissue (Figure 4h). To compare the efficacy of the doxycycline delivery by nanowafer with topical eye drop treatment, another group of mice were treated with doxycycline eye drops. Upon examination under a fluorescence microscope, the corneas did not exhibit a measurable green fluorescence, indicating the complete clearance of the drug within a few minutes (Figure 4i and j). Although, doxycycline concentration was undetectable in tears after 4 h, the fluorescence and intravital confocal imaging studies have confirmed the presence of the drug in the corneal tissue for up to 24 h. Taken together, this study clearly demonstrates the ability of the nanowafer to release doxycycline for an extended period of time, thus enhancing the precorneal drug residence time and subsequent diffusion of drug molecules into the cornea.

Tyrosine Kinase Receptor Inhibitor Drugs to Load into the Nanowafers. TKI drugs were selected as the most suitable candidates for loading into PVA nanowafers and

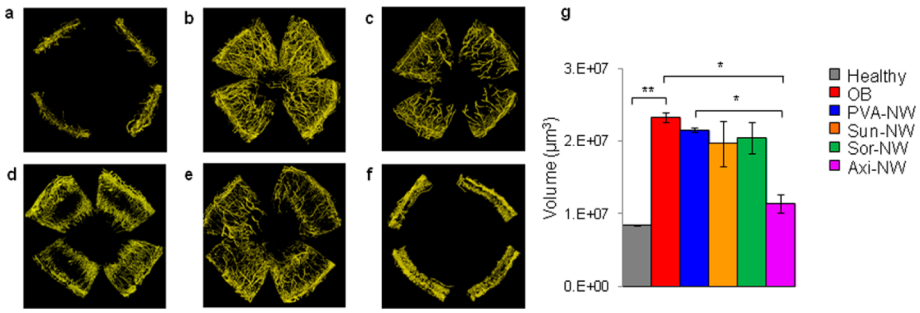

Figure 5. Selection of tyrosine kinase receptor inhibitor drugs. Screening of tyrosine kinase inhibitor drugs loaded nanowafers for their relative therapeutic efficacy in inhibiting corneal neovascularization after 10 days of treatment. Representative 3D reconstructed corneal images of fluorescence confocal microscopy: (a) healthy cornea (control); (b) untreated ocular burn (control); (c) blank PVA-NW; (d) Sora-NW; (e) Suni-NW; (f) Axi-NW. (g) Quantification of corneal neovascularization volume. $n = 3$ animals, *$P < 0.05$ *vs* OB control and $P < 0.05$ *vs* PVA-NW, **$P < 0.01$. All error bars represent standard deviation from the mean.

further evaluated for their relative therapeutic efficacy. The TKI drugs constitute a rapidly evolving class of low molecular weight antiangiogenic drugs that can selectively bind and inhibit the upregulation of tyrosine kinase receptors such as VEGFR1, VEGFR2, PDGFR-A, and PDGFR-B.[36] These drugs are very effective in suppression and regression of neovascularization.[37] Nanowafers containing sunitinib, sorafenib, and axitinib were fabricated for this study. These drugs were chosen, as they are already in clinical use as antiangiogenic therapeutics to treat late-stage renal carcinoma.[38−40]

To select the most suitable drug for the treatment of CNV, PVA nanowafers loaded with sunitinib (Sun-NW), sorafenib (Sor-NW), and axitinib (Axi-NW) were investigated for their relative therapeutic efficacy and compared with untreated OB group and PVA nanowafer (PVA-NW)-treated groups. For mouse experiments, each nanowafer was fabricated to be 2 mm in diameter to exactly cover the corneal surface and contained 5 μg of the drug. The nanowafers were instilled on the cornea immediately after the alkali burn. The mice were subjected to once a day nanowafer treatment for 10 days followed by a 5-day observation period. The CNV was monitored by slit-lamp imaging every other day. This study revealed an extensive neovascularization of the corneas in untreated OB and PVA-NW-treated control groups. The Sun-NW- and Sor-NW-treated groups also exhibited neovasculature. In all these groups, the new blood vessels proliferated from the limbal rim area to the center of the cornea. The Axi-NW-treated corneas were the clearest and had less CNV compared to the untreated OB control group, and the new blood vessels were closely restricted to the limbal area (Supplementary Figure S1). At the end of the treatment period, whole mount specimens of these corneas were prepared and treated with rat anti-mouse CD31 antibody and Alexa-Fluor 594-conjugated goat anti-rat secondary antibody to label vascular endothelium, and subjected to laser scanning confocal fluorescence imaging.[41] This study revealed that Sun-NW and Sora-NW were not very effective in suppressing the CNV. The Axi-NW treatment was the most effective, and the corneas appeared to be almost close to the healthy cornea with minimal CNV restricted to the limbal area (Figure 5a−f). The CNV volume was quantified for each group using the IMARIS program. The Axi-NW-treated group exhibited significantly less CNV compared to the untreated control and PVA-NW groups ($P < 0.05$). The Axi-NW is almost twice as effective as Sun-NW and Sor-NW in suppressing the CNV (Figure 5g). Taken together, these results demonstrated the pronounced therapeutic efficacy of the Axi-NW compared to the untreated control group and also the Sun-NW- and Sor-NW-treated mouse groups. On the basis of these results, Axi-NW was selected for further study.

To minimize the drug-related side effects, the maximum tolerated therapeutic dose was determined by conducting a drug escalation study. Administration of maximum tolerated dose is usually associated with maximum clinical benefit. For this study, nanowafers containing 10, 5, and 2.5 μg of axitinib (Axi-10-NW, Axi-5-NW, and Axi-2.5-NW) were fabricated and tested for their therapeutic efficacy in OB mice. Axi-5-NW and Axi-2.5-NW were the most efficacious compared to Axi-10-NW (Supplementary Figure S2). Both Axi-5-NW and Axi-2.5-NW exhibited almost the same efficacy, and the CNV volumes were significantly lower than the OB control group ($P < 0.01$). Slit-lamp examination revealed no changes in macroscopic appearance of the eyelids or the conjunctiva for 15 days during the Axi-5-NW and Axi-2.5-NW treatment and observation periods when compared with the control groups. There were no drug-related adverse effects of the Axi-5-NW and Axi-2.5-NW treatment. However, in the case of Axi-10-NW treatment, a few corneal perforations were observed after day 3. On the basis of this study, Axi-5-NW was selected as the maximum tolerated dose for comparing the efficacy of nanowafer and eye drop drug delivery methods.

Enhanced Therapeutic Efficacy of Axitinib Nanowafer. Because of the physiological barriers of the ocular surface,

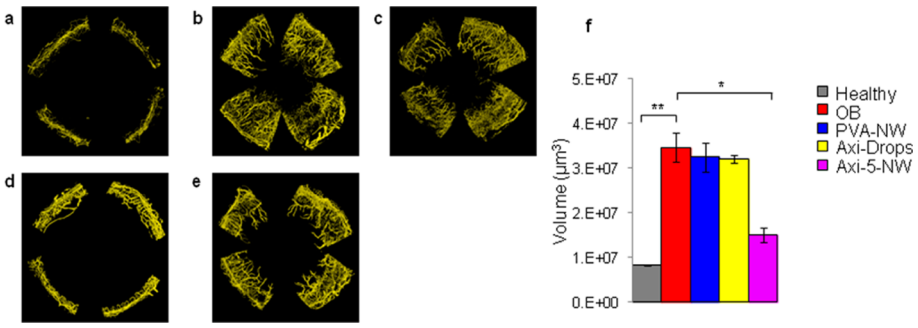

Figure 6. Axitinib nanowafer is more efficacious than the topical eye drop treatment. Representative 3D reconstructed corneal images revealing the enhanced therapeutic efficacy of Axi nanowafer compared to twice a day eye drop treatment. (a) Healthy cornea. (b) OB-induced cornea. (c) PVA-NW. (d) Axi-NW. (e) Twice a day Axi-eye drop (0.1%) treatment. (f) Quantification of corneal neovascularization volume. n = 3 animals, $*P < 0.05$ *vs* OB control. All error bars represent standard deviation from the mean.

topical eye drops must be applied several times a day for a therapeutic effect, thus increasing the potential for toxic side effects. In this study, once a day Axi-5-NW treatment was compared with Axi eye drops (0.1%) administered twice a day for its therapeutic effect in inhibiting CNV in an OB mouse model. A circular Axi-5-NW was placed on the injured cornea under general anesthesia, daily for 10 days followed by 5 days of observation. On the 15th day, the corneas were collected, processed, and subjected to laser scanning fluorescence confocal microscopy.

The images of whole mount corneas clearly demonstrated a strong therapeutic effect of the Axi-5-NW treatment compared to the untreated OB control group (Figure 6a–e). The Axi-5-NW treatment has restricted the proliferation of blood vessels to the limbal area and very closely resembled the healthy uninjured cornea. However, the OB control, PVA-NW, and Axi eye drop treated corneas exhibited an extensive neovascularization. The new blood vessels were highly branched and extended from the limbal area toward the center of the cornea. In the case of Axi-5-NW treatment, the amount of drug delivered to the cornea was 5 μg per day, and for axitinib eye drop treatment it was 10 μg per day. Although, eye drop treated mice received twice the drug dosage as those treated with Axi-5-NW, still Axi-5-NW treatment was twice as efficacious as the eye drop treatment (Figure 6f). These results confirmed that the controlled drug release from Axi-5-NW is more effective in inhibiting CNV compared to the eye drop treatment even at a lower dosing frequency.

To further compare the efficacy of Axi-5-NW and Axi eye drops at the molecular level, expression levels of the drug target factors VEGF-A, VEGF-R1, VEGF-R2, PDGFR-A, PDGFR-B, TNF-α, bFGF, and TGF-β were measured, in addition to proinflammatory interleukins and proangiogenic matrix metalloproteinases. The Axi-NW was much more effective at suppressing Axi-target genes compared to the untreated OB and Axi-eye drop treatment (Figure 7). The Axi-5-NW also showed significant suppression of proinflammatory cytokine and proangiogenic MMP expression compared to OB alone and Axi-eye drops (Supplementary Figure S3). These results reaffirmed the enhanced efficacy of axitinib when delivered by a nanowafer once a day for 10 days compared to the twice a day topical eye drop treatment for the same period of time.

Axitinib Nanowafer Improves Corneal Wound Healing. The effect of Axi-5-NW on the corneal wound healing process was studied by corneal fluorescein staining. This study revealed that the corneal wound healing was unaffected by the Axi-5-NW treatment, and a normal healing pattern was observed. The rate of epithelial closure of the corneal surface was almost the same in both Axi-5-NW and Axi-eye drop treated groups, and complete corneal surface recovery was observed by the ninth day. However, the OB control and PVA-NW-treated groups demonstrated a slightly slower recovery, and complete healing was observed by the 11th day (Figure 8). These results confirmed that axitinib is nontoxic and did not affect the epithelial recovery of the OB-induced corneas, unlike other antiproliferative agents such as mitomycin C and 5-fluorouracil, which are prone to retarding the corneal epithelial recovery.[41]

CONCLUSIONS

Ocular drug delivery systems aim to deliver the pharmacologic agent at the desired therapeutic concentration to the target ocular tissue without damaging the healthy tissue. In the treatment of ocular disease, however, this aim becomes more challenging because of the protective ocular surface barriers and highly sensitive ocular tissues. The challenge is to delicately circumvent these protective ocular surface barriers and deliver the drug to the target site (cornea or conjunctiva) without causing permanent tissue damage. Despite sustained efforts, the development and optimization of new nano drug delivery systems have been very slow. To improve the therapeutic efficacy of ophthalmic drugs, the drug delivery system

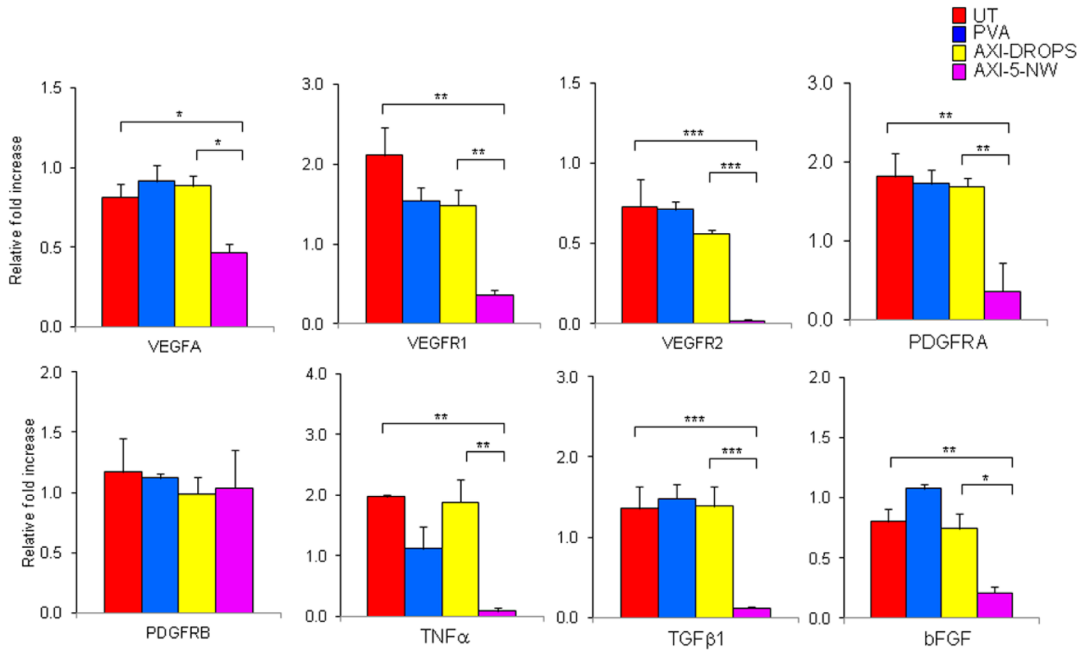

Figure 7. Enhanced therapeutic effect of axitinib nanowafer. RT-PCR analysis revealing the strong suppression of the expression levels of drug target genes by nanowafer compared to twice a day topical axitinib eye drop treatment. *n* = 3 (5 animals per group). **P* < 0.05, ***P* < 0.01, ****P* < 0.001. All error bars represent standard deviation from the mean.

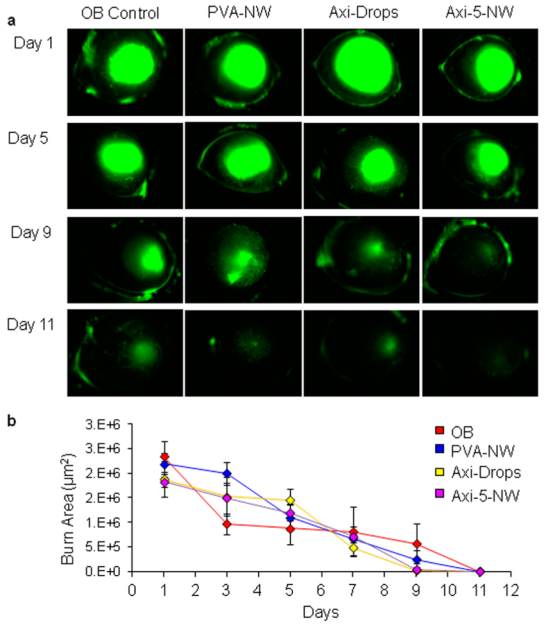

Figure 8. Axitinib nanowafer treatment improves the corneal wound healing after ocular burn injury. (a) Fluorescence images. (b) Plot demonstrating corneal surface healing as a measure fluorescence intensity. *n* = 3 animals. All error bars represent standard deviation from the mean.

should be able to release the drug in a controlled fashion, increase drug residence time on the ocular surface, improve the bioavailability of the drug, and improve the local tolerability of the drug. Also, the issue of patient compliance must be seriously considered in ocular drug delivery. For example, if a drug must be given 4–8 times a day for a week when treating a chronic disease, it is very unlikely to be given in a timely fashion. Therefore, development of a controlled release ocular drug delivery system that can release the drug in therapeutically effective concentrations for a longer duration of time (from a day to a week) is highly desired.

This work presents a nanowafer drug delivery platform involving the seamless integration of nanofabrication and drug delivery technologies. A systematic screening of a series of polymers confirmed that PVA is a nonimmunostimulatory polymer that can be used in the fabrication of ocular drug delivery nanowafers, wherein PVA and the drug axitinib work synergistically. The laser scanning confocal imaging and RT-PCR studies have quantitatively demonstrated the enhanced therapeutic efficacy of the nanowafer in terms of inhibiting neovascularization and improved suppression of proinflammatory and proangiogenic factors in an ocular burn induced mouse model. The nanowafer has demonstrated an enhanced efficacy compared to topically applied eye drop treatment. This study also demonstrated that the enhanced therapeutic efficacy is due to the increased drug residence time on the ocular surface, which subsequently diffused into the ocular tissue for therapeutic action. The additive effects of negligible inflammatory potential, mucoadhesivity, controlled drug release, and the therapeutic potential of the drug support the development of a broadly applicable synergistic nanowafer drug delivery system. Furthermore, the nanowafer, at the end of the stipulated drug release time, will dissolve and fade away. The simplicity and efficiency of the nanowafer drug

delivery system provides a new and novel modality for the noninvasive drug administration to the ocular surface. The nanowafer drug delivery system can deliver a wide range of drugs regardless of molecular weight or chemical properties. Development of a nanowafer drug delivery system that can be readily instilled on the ocular surface by the patient's fingertip without any clinical procedure will be not only very convenient but also most desirable for treating eye injuries, infections, chronic dry eye, glaucoma, and other ocular inflammatory conditions. Since, the polymers and drugs used in the development of the nanowafer are already in clinical use, it can be rapidly translated to the clinic for human trials.

MATERIALS AND METHODS

All animals were treated in accordance with the Association of Research in Vision and Ophthalmology (ARVO) Statement for the Use of Animals in Ophthalmic and Vision Research, and the protocols were approved by the Baylor College of Medicine Institutional Animal Care and Use Committee.

Nanowafer Fabrication. Silicon wafers having wells of 500 nm diameter and 500 nm depth were fabricated by e-beam lithography and dry reactive ion etching following a previously published procedure.[23,24] By using the silicon wafer as a master template, poly(dimethylsiloxane) imprints were fabricated. A clear PVA solution (5% w/v) was prepared by dissolving PVA (5 g) in 100 mL of a water/ethanol mixture (4:6) on a stirring hot plate at 70 °C (RT Elite stirring hot plate, Fisher Scientific) until a clear homogeneous solution was formed. Thus, the prepared PVA solution (5 mL) was transferred with a pipet onto a 3 in. diameter PDMS template containing vertical posts and kept in an oven (Isotemp 500 Series Economy Lab Ovens, Fisher Scientific) at 60 °C for 30 min. This procedure resulted in the formation of PVA nanowafers having 500 nm wells. The 500 nm wells in the PVA nanowafer were filled with Axitinib/PVA solution. The Axitinib/PVA solution was prepared by dissolving Axitinib (100 mg in 250 μL of DMSO) in 750 μL of 5% PVA solution. Thus, the prepared Axitinib/PVA solution (200 μL) was transferred onto a PVA nanowafer (3 in. diameter), swiped with a razor blade to fill the wells, and left at room temperature to evaporate the solvent.[27] The drug-filled hydrogel templates were cut into 2 mm diameter discs with a paper punch. The drug content in 2 mm nanowafers was evaluated by HPLC. The nanowafers thus prepared were used for *in vivo* experiments in mice.

Doxy Nanowafer Instillation, Imaging, and Tear Collection. A nanowafer was placed on top of each cornea with a forceps while observing under a stereomicroscope followed by wetting with 5 μL of balanced salt solution (BSS). The mice were anesthetized by ketamine (100 mg/kg) and xylazine (10 mg/kg) injection. The nanowafers dissolved in approximately half an hour. Since doxycycline is a fluorescent drug, Doxy nanowafers were monitored hourly for 5 h *via* imaging in a stereoscopic zoom microscope (model SMZ 1500; Nikon, Melville, NY, USA), with a fluorescence excitation at 470 nm.

Tear fluid was collected at regular intervals by instilling 2 μL of BSS on the ocular surface. After a few seconds the tears were collected from the conjunctival sac close to the lacrimal punctum.[35] The tear fluid and isotonic solution were collected with a 1 μL volume glass capillary tube (Drummond Scientific, Broomhall, PA, USA) by capillary action from the interior tear meniscus in the lateral canthus. The tear washings from a group of 15 mice were pooled, centrifuged, and stored at −80 °C prior to HPLC analysis to determine the drug concentration.

Intravital Imaging of Doxy Nanowafers. Mice instilled with doxycycline nanowafers after 24 h were anesthetized with ketamine and xyalizine and imaged under a Nikon ECLIPSE intravital microscope (Nikon, Melville, NY, USA). Images were captured with a resolution of 1024 × 768 pixels with X10 Nikon objectives.

HPLC Analysis. HPLC experiments were performed on a Shimadzu Prominence HPLC system. The analytical column was a Kinetex 5uXB-C18 100A (150 mm × 4.6 mm) from Phenomenex. The system was equipped with autosampler, in-line degasser, and column oven set at room temperature. The mobile phase for doxycycline analysis was a mixture of 5% acetic acid (55%) and methanol (45%) (Sigma-Aldrich, St. Louis, MO, USA). Injection volume was 5 μL, the flow rate was 1.0 mL/min, and the pressure was lower than 2500 psi.

Determination of total drug content in a nanowafer: The total amount of a drug loaded in the nanowafer was determined by dissolving an accurately weighed nanowafer in 1 mL of PBS solution, followed by addition of 2 mL of ethanol. The precipitated polymer was removed by centrifugation. The clear solution was filtered through a 0.2 μm syringe filter, analyzed by UV-HPLC, and compared with the standard curve to quantify the total drug content in the nanowafer. This experiment was performed in triplicates.

Study of drug release kinetics of the nanowafers by HPLC analysis: Each sample was filtered through a 0.2 μm syringe filter and subjected to HPLC analysis. The UV detection wavelength for doxycycline was 274 nm. The drug concentration was calculated by comparing the peak area of standards and sample.

Ocular Burn Mouse Model and Nanowafer Treatment. Naive female C57BL/c mice 6 to 8 weeks of age (The Jackson Laboratory, Bar Harbor, ME, USA) were anesthetized with an intraperitoneal injection of the rodent combination anesthesia previously mentioned, combined with topical anesthesia of the right eyes by 0.5% proparacaine. Whatman filter paper (2.5 mm diameter) was briefly soaked in 1 N NaOH solution and then placed on the right corneas for 30 s and then rinsed with 20 mL of BSS. Mice corneas were monitored daily using a slit lamp microscope (model 30-99-49, Zeiss, Oberkochen, Germany) for 14 days, and images were recorded by an attached Nikon D40X digital camera. For treatment, each day a specific nanowafer was placed on top of the ocular burn cornea of an anesthetized mouse corresponding to the treatment group. All mice then received 5 μL of BSS on the ocular burn cornea, including control groups.

Corneal Fluorescein Staining. The extent of corneal wound closure was examined by corneal fluorescein staining. On days 1, 3, 5, 7, 9, and 11 after ocular burn, mice were anesthetized with an intraperitoneal injection of the above-mentioned rodent combination anesthesia. A 1 μL amount of fluorescein (0.1%) was instilled on the ocular burn corneas for 1 min, followed by rinsing with 1 mL of BSS. Images were recorded by a stereoscopic zoom microscope (model SMZ 1500; Nikon), with a fluorescence excitation at 470 nm.

Corneal Whole Mount Staining. Fourteen days after the ocular burn, eyes were enucleated for corneal whole mount staining with some modifications.[42] Briefly, corneas including limbal area were dissected from freshly enucleated eyes, and surrounding conjunctiva, Tenon capsule, uvea, and lens were carefully removed, followed by making four slits with a scalpel blade at 90°, 180°, 270°, and 360° to flatten out the corneas, then fixed in 4% (wt/vol) paraformaldehyde solution at room temperature for 1 h. Tissues were blocked with 10% goat serum and 0.5% Triton X-100 prepared in PBS for 1 h. Rat anti-mouse CD31 antibody (1:300) (BD Biosciences, San Jose, CA, USA) supplemented with 5% goat serum and 0.1% Triton X-100 was added to the tissues and allowed to incubate at 4 °C for 3 days. After a series of washing with PBS and blocking with the above-mentioned solution, the tissues were incubated with Alexa-Fluor 594-conjugated goat anti-rat secondary antibody (Jackson ImmunoResearch, West Grove, PA, USA) in a dark chamber for 1 h at room temperature. The tissues were then mounted on slides using Fluoromount G (Southern Biotech, Birmingham, AL, USA) containing DAPI (1:300) (Life Technologies, Grand Island, NY, USA).

Laser Confocal Fluorescence Imaging and 3D Representations of Whole-Mounted Corneas. Images of whole-mounted corneas were obtained by stitching individual Z-stack images (~11 × 11) acquired in a Nikon Eclipse Ni confocal microscope provided with a 20× objective (Plan APO20X-0.75/OFN25-DIC-N2 by Nikon) and a 561 nm laser (blood vessel detection, red). Each Z-stack was captured using nonresonant galvano scanners, 512 × 512 pixel size, unidirectional scan, 0.5 scan speed, 2.2 pixel dwell, 0.9 μm Z-space, and 19.2 μm pinhole size. Images were stitched by NIS Elements software, and some of them were deconvolved in the NIS Deconvolution module in order to improve the signal. Images were further processed with IMARIS 7.7.2 (Bitplane AG, Zurich, Switzerland) software for 3D representations and volume calculations. Confocal images were masked using the surpass mode, and the surface function set it up with 3.0 μm surface grain size and 10 μm for the diameter of the largest sphere parameters. The thresholds were adjusted manually for each image. Blood vessel volumes of the 3D representations were calculated using the Statistic function. Data in figures are shown as mean ± SEM of each treatment repeated in triplicates. Statistical significance of comparison of mean values was assessed by one-way-ANOVA followed by Tukey's test for multiple comparisons. Mean differences of the groups were considered significant at $^{*}P < 0.05$, $^{**}P < 0.01$, and $^{***}P < 0.001$.

Quantitative Reverse Transcription–Polymerase Chain Reaction. Mice were sacrificed 5 days after OB with different treatment. After enucleating, corneas were excised and dissected from surrounding conjunctiva and uvea. Pools of five corneas were prepared in triplicate for each treating group. RNA was extracted by a previously reported procedure with RNeasy MicroKit columns (Qiagen, Valencia, CA, USA).[43] Samples were treated with DNase (Qiagen) and stored at −80 °C. The first-strand cDNA was synthesized from 1.0 μg of RNA with Ready-To-Go You-Prime First-Strand Beads (GE Healthcare, Princeton, NJ, USA) and random hexamers (Applied Biosystems, Foster City, CA, USA). RT-PCR was performed using TaqMan Gene Expression Master Mix and Assays (Applied Biosystems). Specific primers from Applied Biosystems were used to quantify gene expression levels. The threshold cycle for each target mRNA was normalized to glyceraldehyde-3-phosphate dehydrogenase mRNA and averaged. Three groups of five-cornea pools were processed for each group.

Conflict of Interest: The authors declare no competing financial interest.

Supporting Information Available: Slit-lamp images of the ocular burn induced corneas demonstrating the therapeutic effect of the drug nanowafers on corneal neovascularization; drug escalation study to determine the maximum tolerated drug dose in the nanowafer; and the PCR data demonstrating the nonimmunogenic nature of the Axi nanowafer. This material is available free of charge *via* the Internet at http://pubs.acs.org.

Acknowledgment. This work was supported by a grant from the Department of Defense (Award No. 1W81XWH-13-1-0146).

REFERENCES AND NOTES

1. Eye health statistics at a glance. Compiled by American Academy of Ophthalmology. April 2011. http://www.aao.org/newsroom/upload/Eye-Health-Statistics-April-2011.pdf.
2. Azar, D. T. Corneal Angiogenic Privilege: Angiogenic and Antiangiogenic Factors in Corneal Avascularity, Vasculogenesis, and Wound Healing. *Trans. Am. Ophthalmol. Soc.* **2006**, *104*, 264–302.
3. Urtti, A. Challenges and Obstacles of Ocular Pharmacokinetics and Drug Delivery. *Adv. Drug Delivery Rev.* **2006**, *58*, 1131–1135.
4. Novack, G. D. Ophthalmic Drug Delivery: Development and Regulatory Considerations. *Clin. Pharmacol. Ther.* **2009**, *85*, 539–543.
5. Kim, Y. C.; Chiang, B.; Wu, X.; Prausnitz, M. R. Ocular Delivery of Macromolecules. *J. Controlled Release* **2014**, *190*, 172–181.
6. Mannermaa, E.; Vellonen, K.-S.; Urtti, A. Drug Transport in Corneal Epithelium and Blood–Retina Barrier: Emerging Role of Transporters in Ocular Pharmacokinetics. *Adv. Drug Delivery Rev.* **2006**, *58*, 1136–1163.
7. Salminen, L. Review: Systemic Absorption of Topically Applied Ocular Drugs in Humans. *J. Ocul. Pharmacol.* **1990**, *6*, 243–249.
8. Baudouin, C. Side Effects of Antiglaucomatous Drugs on the Ocular Surface. *Curr. Opin. Ophthalmol.* **1996**, *7*, 80–86.
9. Topalkara, A. C.; Guler, C.; Arici, D. S.; Arici, M. K. Adverse Effects of Topical Antiglaucoma Drugs on the Ocular Surface. *Clin. Exp. Ophthalmol.* **2000**, *28*, 113–117.
10. Hoffart, L.; Matonti, F.; Conrath, J.; Daniel, L.; Ridings, B.; Masson, G. S.; Chavane, F. Inhibition of Corneal Neovascularization after Alkali Burn: Comparison of Different Doses of Bevacizumab in Monotherapy or Associated with Dexamethasone. *Clin. Exp. Ophthalmol.* **2010**, *38*, 346–352.
11. Mello, G. R.; Pizzolatti, M. L.; Wasilewski, D.; Santhiago, M. R.; Budel, V.; Moreira, H. The Effect of Subconjunctival Bevacizumab on Corneal Neovascularization, Inflammation and Re-epithelization in a Rabbit Model. *Clinics* **2011**, *66*, 1443–1449.
12. Diebold, Y.; Calonge, M. Applications of Nanoparticles in Ophthalmology. *Prog. Retina Eye Res.* **2010**, *29*, 596–609.
13. Gershkovich, P.; Wasan, K. M.; Barta, C. A. A Review of the Application of Lipid-Based Systems in Systemic, Dermal, Transdermal, and Ocular Drug Delivery. *Crit. Rev. Ther. Drug* **2008**, *25*, 545–584.
14. Choy, Y. B.; Park, J.-H.; McCarey, B. E.; Edelhauser, H. F.; Prausnitz, M. R. Mucoadhesive Microdiscs Engineered for Ophthalmic Drug Delivery: Effect of Particle Geometry and Formulation on Preocular Residence Time. *Invest. Ophthalmol. Vis. Sci.* **2008**, *49*, 4808–4815.
15. Chang, E.; McClellan, A. J.; Farley, W. J.; Li, D.-Q.; Pflugfelder, S. C.; De Paiva, C. Biodegradable PLGA-Based Drug Delivery Systems for Modulating Ocular Surface Disease under Experimental Murine Dry Eye. *J. Clin. Exp. Ophthalmol.* **2011**, *2*, 191.
16. He, C.; Kim, S. W.; Lee, D. S. *In Situ* Gelling Stimuli-Sensitive Block Copolymer Hydrogels for Drug Delivery. *J. Controlled Release* **2008**, *127*, 189–207.
17. Gulsen, D.; Chauhan, A. Ophthalmic Drug Delivery through Contact Lenses. *Invest. Ophthalmol. Vis. Sci.* **2004**, *45*, 2342–2347.
18. Singh, K.; Nair, A. B.; Kumar, A.; Kumria, R. Novel Approaches in Formulation and Drug Delivery using Contact Lenses. *J. Basic Clin. Pharm.* **2011**, *2*, 87–101.
19. Shin, Y. J.; Hyon, J. Y.; Choi, W. S.; Yi, K.; Chung, E.-S.; Chung, T.-Y.; Wee, W. R. Chemical Injury-Induced Corneal Opacity and Neovascularization Reduced by Rapamycin *via* TGF-β1/ERK Pathways Regulation. *Invest. Ophthalmol. Vis. Sci.* **2013**, *54*, 4452–4458.
20. Ludwig, A. The Use of Mucoadhesive Polymers in Ocular Drug Delivery. *Adv. Drug Delivery Rev.* **2005**, *57*, 1595–1639.
21. Moshirfar, M.; Pierson, K.; Hanamaikai, K.; Santiago-Caban, L.; Muthappan, V.; Passi, S. F. Artificial Tears Potpourri: A Literature Review. *Clin. Ophthalmol.* **2014**, *8*, 1419–1433.
22. Aragona, P.; Spinella, R.; Rania, L.; Postorino, E.; Sommario, M. S.; Roszkowska, A. M.; Puzzolo, D. Safety and Efficacy of 0.1% Clobetasone butyrate Eyedrops in the Treatment of Dry Eye in Sjögren Syndrome. *Eur. J. Ophthalmol.* **2013**, *23*, 368–376.
23. Acharya, G.; Shin, C. S.; McDermott, M.; Mishra, H.; Park, H.; Kwon, I. C.; Park, K. The Hydrogel Template Method for Fabrication of Homogeneous Nano/Micro Particles. *J. Controlled Release* **2010**, *141*, 314–319.
24. Acharya, G.; Shin, C. S.; Vedantham, K.; McDermott, M.; Rish, T.; Hansen, K.; Fu, Y.; Park, K. A Study of Drug Release from Homogeneous PLGA Microstructures. *J. Controlled Release* **2010**, *146*, 201–206.
25. Streilein, J. W. Ocular Immune Privilege: The Eye Takes a Dim but Practical View of Immunity and Inflammation. *J. Leukoc. Biol.* **2003**, *74*, 179–185.
26. Sivak, J. M.; Ostriker, A. C.; Woolfenden, A.; Demirs, J.; Cepeda, R.; Long, D.; Anderson, K.; Jaffee, B. Pharmacologic

Uncoupling of Angiogenesis and Inflammation During Initiation of Pathological Corneal Neovascularization. *J. Biol. Chem.* **2011**, *286*, 44965–44975.
27. Dobrovolskaia, M. A.; Mcneil, S. E. Immunological Properties of Engineered Nanomaerials. *Nat. Nanotechnol.* **2007**, *2*, 469–478.
28. Zolinik, B. S.; Gonzalez-Fernandez, A.; Sadrieh, N.; Dobrovolskaia, M. A. Nanoparticles and the Immune System. *Endocrinology* **2010**, *151*, 458–465.
29. Smith, D. M.; Simon, J. K.; Baker, J. R., Jr. Applications of Nanotechnology for Immunology. *Nat. Rev. Immunol.* **2013**, *13*, 592–605.
30. Barrientos, S.; Stojadinovic, O.; Golinko, M. S.; Brem, H.; Tomic-Canic, M. Growth Factors and Cytokines in Wound Healing. *Wound Rep. Reg.* **2008**, *16*, 585–601.
31. Qazi, Y.; Maddula, S.; Ambati, B. K. Mediators of Ocular Angiogenesis. *J. Genet.* **2009**, *88*, 495–515.
32. Ellenberg, D.; Azar, D. T.; Hallak, J. A.; Tobaigy, F.; Han, K. Y.; Jain, S.; Zhou, Z.; Chang, J.-H. Novel Aspects of Corneal Angiogenic and Lymphangiogenic Privilege. *Prog. Retinal Eye Res.* **2010**, *29*, 208–248.
33. Maddula, S.; Davis, D. K.; Maddula, S.; Burrow, M. K.; Ambati, B. K. Horizons in Therapy for Corneal Angiogenesis. *Ophthalmology* **2011**, *118*, 591–599.
34. Liss, R. H.; Norman, J. C. Visualization of Doxycycline in Lung Tissue and Sinus Secretions by Fluorescent Techniques. *Chemotherapy* **1975**, *21* (Suppl 1), 27–35.
35. Corrales, R. M.; Villarreal, A.; Farley, W.; Stern, M. E.; Li, D.-Q.; Pflugfelder, S. C. Strain-Related Cytokine Profiles on the Murine Ocular Surface in Response to Desiccating Stress. *Cornea* **2007**, *26*, 579–584.
36. Shawver, L. K.; Slamon, D.; Ullrich, A. Smart Drugs: Tyrosine Kinase Inhibitors in Cancer Therapy. *Cancer Cell* **2002**, *1*, 117–123.
37. Ribatti, D. Tyrosine Kinase Inhibitors as Antiangiogenic Drugs in Multiple Myeloma. *Pharmaceuticals* **2010**, *3*, 1225–1231.
38. Motzer, R. J.; Hutson, T. E.; Tomczak, P.; Michaelson, M. D.; Bukowski, R. M.; Rixe, O.; Oudard, S.; Negrier, S.; Szczylik, C.; Kim, S. T.; *et al*. Sunitinib *versus* Interferon *alfa* in Metastatic Renal Cell Carcinoma. *N. Engl. J. Med.* **2007**, *356*, 115–124.
39. Escudier, B.; Eisen, T.; Stadler, W. M.; Szczylik, C.; Oudard, S.; Siebels, M.; Negrier, S.; Chevreau, C.; Solska, E.; Desai, A. A.; *et al*. Sorafenib in Advanced Clear-Cell Renal-Cell Carcinoma. *N. Engl. J. Med.* **2007**, *356*, 125–134.
40. Gross-Goupil, M.; Francois, L.; Quivy, A.; Ravaud, A. Axitinib: A Review of its Safety and Efficacy in the Treatment of Adults with Advanced Renal Cell Carcinoma. *Clin. Med. Insights Oncol.* **2013**, *7*, 269–277.
41. Ando, H.; Ido, T.; Kawai, Y.; Yamamoto, T.; Kitazawa, Y. Inhibition of Corneal Epithelial Wound Healing: A Comparative Study of Mitomycin C and 5-Fluorouracil. *Ophthalmology* **1992**, *99*, 1809–1814.
42. Cao, R.; Lim, S.; Ji, H.; Zhang, Y.; Yang, Y.; Honek, J.; Hedlund, E.-M.; Cao, Y. Mouse Corneal Lymphangiogenesis Model. *Nat. Protoc.* **2011**, *6*, 817–826.
43. Yuan, X.; Mitchell, B. M.; Wilhelmus, K. R. Expression of Matrix Metalloproteinases during Experimental Candida albicans keratitis. *Invest. Ophthalmol. Vis. Sci.* **2009**, *50*, 737–742.